ACS APPLIED MATERIALS & INTERFACES

Research Article

www.acsami.org

Electrospun Fibrous Mats with Conjugated Tetraphenylethylene and Mannose for Sensitive Turn-On Fluorescent Sensing of *Escherichia coli*

Long Zhao, Yufei Chen, Jiang Yuan, Maohua Chen, Hong Zhang, and Xiaohong Li*

Key Laboratory of Advanced Technologies of Materials, Ministry of Education, School of Materials Science and Engineering, Southwest Jiaotong University, Chengdu 610031, P.R. China

ABSTRACT: A rapid and sensitive detection of microbes in water and biological fluids is a key requirement in water and food safety, environmental monitoring, and clinical diagnosis and treatment. In the current study, electrospun polystyrene-*co*-maleic anhydride (PSMA) fibers with conjugated mannose and tetraphenylethylene (TPE) were developed for *Escherichia coli* (*E. coli*) detection, taking advantage of the high grafting capabilities of ultrafine fibers and the highly porous structure of the fibrous mat to entrap bacterial cells. The specific binding between mannose grafts on PSMA fibers and FimH proteins from the fimbriae of *E. coli* led to an efficient "turn-on" profile of TPE due to the aggregation-induced emission (AIE) effect. Poly(ethylene glycol) diamine was used as hydrophilic tethers to increase the conformational mobility of mannose grafts, indicating a more sensitive change in the fluorescence intensity against bacteria concentrations, a lower fluorescence background of fibers without bacteria incubation, and a sufficient space for bacteria binding, compared with the use of hexamethylenediamine or poly(ethylene imine) as spacers for mannose grafting. The addition of bovine serum albumin, glucose, or both of them into bacteria suspensions showed no significant changes in the fluorescence intensity of fibrous mats, indicating the anti-interference capability against these proteins and saccharides. An equation was drafted of the fluorescence intensities of fibrous mats against *E. coli* concentrations ranging from 10^2 to 10^5 CFU/mL. The test strip format was established on mannose-conjugated PSMA fibers after exposure to *E. coli* of different concentrations, providing a potential tool with a visual sensitivity of bacteria concentrations as low as 10^2 CFU/mL in a matter of minutes. This strategy may offer a capacity to be expanded to exploit electrospun fibrous mats and other carbohydrate−cell interactions for bioanalysis and biosensing of pathogenic bacteria.

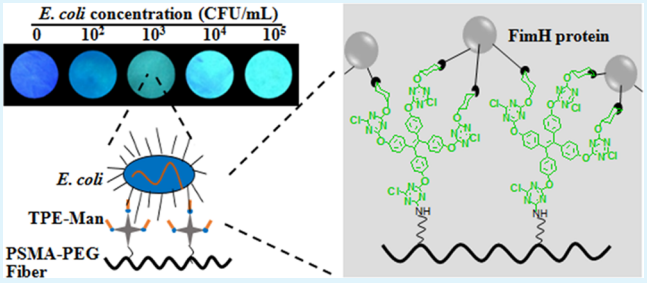

KEYWORDS: *electrospun fibrous mat, tetraphenylethylene, aggregation-induced emission, bacterium detection, bacterium testing strip*

1. INTRODUCTION

Nowadays, one of the challenges to human health is the constant threat from existing and emerging infectious diseases. Bacterial contamination of food, water, and air is becoming a continuous and expanding problem worldwide as a result of global climate change and environmental pollution. Bacterial infections cause 300 million cases of severe illness each year, and over 3 million people die from microbial intestinal infections per year. Particularly, poor waterbody sanitation leads to more susceptible individuals exposed to pathogen-contaminated water and food in many developing countries, where microbial infections constitute the major causes of death.[1] Therefore, a rapid and sensitive detection of microbes in water and biological fluids is a key requirement in food safety, environmental monitoring, and clinical diagnosis and treatment.

Currently, various available methods exist for bacteria detection, such as plating and culturing, and polymerase chain reaction (PCR). Conventional culture methods are based on bacteria growth on agar media followed by counting the number of colonies formed, which is reliable but time-consuming (at least 1−2 days).[2] PCR-based methods are applied most frequently for bacteria detection with a high selectivity and sensitivity but often require an expensive apparatus and complicated procedures.[3] It should be noted that these methods suffer from extensive sample preparation steps and the requirement of trained operators. Thus, an analysis on the whole bacterium without going through biochemical preparations is highly preferred. For example, biomarkers on the bacterial cell surface are accessible for bacteria detection through antibody−antigen recognitions or other specific ligand−receptor interactions.[4] Ravindranath et al. used magnetic nanoparticles conjugated with antibacteria antibodies that could specifically label target organisms, which were detected later by a portable mid-infrared spectrometer.[5] Lee et al. developed vancomycin-functionalized magnetic nanoparticles that bound with D-alanyl-D-alanine moieties in the bacterial wall and were detected by a diagnostic magnetic

Received: October 31, 2014
Accepted: February 18, 2015
Published: February 18, 2015

DOI: 10.1021/am507593p
ACS Appl. Mater. Interfaces 2015, 7, 5177−5186

resonance system using magnetic particles as a proximity sensor to amplify the molecular interactions, indicating a relaxation time decrease in a concentration-dependent fashion.[6] However, in many cases where the surface characteristics of bacteria may not be previously identified, the specific ligands such as antibodies or ligands might not be effective. Alternatively, the electrostatic interaction with the cell surface has been utilized for bacterial detection. Miranda et al. used gold nanoparticles with quaternary amine headgroups to bind with β-galactosidase, inhibiting the enzymatic activities. The electrostatic binding of negatively charged bacteria to the cationic particle surface displaced β-galactosidase and restored the enzyme activities, providing an enzyme-amplified colorimetric readout of the binding event.[7] Phillips et al. developed noncovalent conjugates of anionic poly(*para*-phenylene ethynylene) with ammonium-functionalized gold nanoparticles to afford fluorescence-quenched complexes. Fluorescent signals were generated in aqueous media upon displacement of the anionic polymer from the nanoparticle surface by bacteria.[8]

The fluorescence-based techniques have advantages of high sensitivity and low background noise over other analytical methods, and various fluorescent materials including proteins and inorganic nanoparticles have been used as fluorescent probes.[9] However, many of these fluorescent materials often suffer from obvious disadvantages, such as low photobleaching thresholds and aggregation-caused quenching, resulting in drastic reductions in their fluorescent signals and intrinsic limitations in the development of efficient bioprobes and biosensors.[10] To overcome these problems, fluorescent materials have recently been developed with aggregation-induced emission (AIE) characteristics, which can greatly improve the fluorescence quantum yields by up to 3 orders of magnitude.[11] As one representative AIE material, tetraphenylethylene (TPE) and its derivatives have displayed extensive application potential in optoelectronic materials and sensors due to their efficient preparation and facile functionalization.[10] The rotation of the phenyl rings of TPE molecules is restricted in the aggregated state due to the physical constraint, which blocks the nonradiative pathways and becomes highly emissive fluorescent molecules.[12] Kato et al. developed fluorescent oligosaccharide probes using TPE derivatives for the detection of virus, toxin, and lectin.[13] Li et al. fabricated polyion complex micelles from cationic polyelectrolyte and negatively charged multivalent TPE sulfonate derivatives, emitting intense fluorescence owing to the AIE effect. After exposure to bacterial cells, the competitive electrostatic binding of the negatively charged bacteria surface with the cationic polyelectrolyte led to a disruption of the micelles and accordingly a decrease of TPE fluorescence intensities due to the loss of AIE effect.[14]

Electrospinning has been used as an efficient processing method for manufacturing unwoven fibrous mats with controllable fiber sizes. Compared to conventional planar materials, electrospun fibers provide a large surface area, leading to a high availability of graft sites and an increase in the reaction rate for developing high-performance biosensor applications.[15] In our previous study, alcohol oxidase, a multimeric enzyme consisting of eight identical subunits, was immobilized on electrospun polystyrene-*co*-maleic anhydride (PSMA) fibers for valid tests of alcoholic saliva, indicating high sensitivity and reusability.[16] In addition, the open and interconnective pore networks of electrospun fibrous mat enable an easy and rapid filtration capability for particles or microbes.[17] Luo et al. developed electrospun membrane nanostructures as a capillary flow substrate and also as a pathogen capture pad in a biosensor, which improved bacteria capture and facilitated assay kinetics.[18]

Escherichia coli (*E. coli*) is frequently associated with a number of infectious diseases, causing various intestinal or extraintestinal infections, such as diarrhea, food poisoning, and urinary tract infections.[19] The presence of *E. coli* is currently considered as an indicator of microbiological quality deterioration, and an accurate routine testing is crucial for the outbreak prevention. Like most other Gram-negative pathogens, *E. coli* establishes infections after adhering to host tissues through interactions between bacterial fimbria and mannose moieties from the host cell surface.[20] FimH is a two-domain adhesion protein at the end of a fimbria, and the sugar-binding properties of FimH proteins have been exploited for an effective detection of *E. coli*. Xue et al. incubated *E. coli* with a mannose-bearing glycopolymer, resulting in the formation of fluorescent cell clusters and significant red shifts in ultraviolet absorption and fluorescent spectra of the polymer.[21] In addition, the weakness of mannose−FimH interactions requires the attachment of a single *E. coli* cell to several mannose molecules for an efficient complex formation.[19] In the current study, the conjugate of TPE and mannose (TPE-Man) was grafted on electrospun fibers for detection of *E. coli* in aqueous solution, taking advantage of the high grafting capabilities of ultrafine fibers and the highly porous structure of the fibrous mat to entrap bacterial cells. The specific binding between mannose grafts on PSMA fibers and FimH proteins from the fimbriae of *E. coli* led to an efficient "turn-on" profile of TPE due to the AIE effect, inducing the fluorescence change of electrospun fibrous mat. The specificity and anti-interference capability for bacteria detection were also evaluated.

2. EXPERIMENTAL SECTION

2.1. Materials. PSMA (M_w = 170 kDa, maleic anhydride content = 14.8 wt %) and polystyrene (PS, M_w = 400 kDa) were obtained from Shanghai Zhaocheng Scientific Development Corp (Shanghai, China). Poly(ethylene imine) (PEI, M_w = 25 kDa), poly(ethylene glycol) (PEG) diamine (M_w = 2 kDa), hexamethylenediamine (HDA), *N*,*N*-diisopropylethylamine (DIPEA), 4,4′-dihydroxybenzophenone, and cyanuric chloride were purchased from Sigma (St Louis, MO). *E. coli* (CMCC 44103) was procured from the Chinese Medical Culture Collection Center (Beijing, China), and *Staphylococcus epidermidis* (*S. epidermidis*, ATCC 12228) was from the American Type Culture Collection (Rockville, MD). Bovine serum albumin (BSA), mannose, and glucose were from Baoxin Biotechnology Co., Ltd. (Chengdu, China). All other chemicals were analytical grade and received from Changzheng Regents Company (Chengdu, China), unless otherwise indicated. Tetrahydrofuran (THF) was purified by distillation from sodium/benzophenone under nitrogen prior to use.

2.2. Synthesis of TPE-Cyanuric Chloride Conjugate. Figure 1A shows the synthetic route for TPE−cyanuric chloride (TPEC) conjugate. Tetrakis(4-hydroxytetraphenyl)ethane (TPE-OH) was synthesized from 4,4′-dihydroxybenzophenone by a McMurry reaction as described previously.[22] Briefly, $TiCl_4$ (1.56 mL, 14.0 mmol) was added dropwise into a stirred suspension of Zn powder (1.84 g, 28.0 mmol) in 70 mL of dry THF below −10 °C. After refluxing under an argon atmosphere for 3 h, 4,4′-dihydroxybenzophenone (3.0 g, 14.0 mmol) solution in dry THF (30 mL) was added to the above suspension, which was refluxed for an additional 4 h. The reaction mixture was cooled to 25 °C and poured into 10% K_2CO_3 aqueous solution. After vigorous stirring for 5 min, the dispersed insoluble material was removed by vacuum filtration, and the aqueous layer was extracted three times with ethyl acetate, which was combined as the organic fraction. After water wash and Na_2SO_4 drying, the solvents

DOI: 10.1021/am507593p
ACS Appl. Mater. Interfaces 2015, 7, 5177−5186

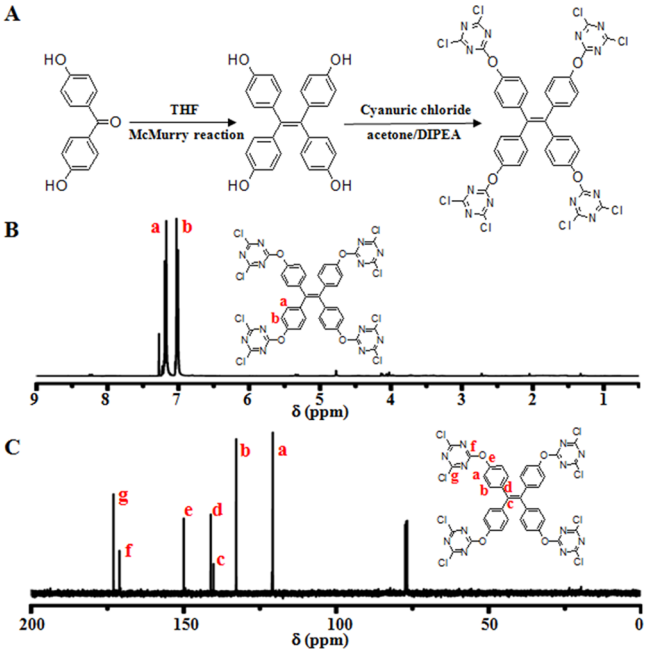

Figure 1. (A) Synthetic route for TPE-OH from 4,4′-dihydroxybenzophenone by a McMurry reaction, followed by conjugation with cyanuric chloride to obtain TPEC. (B) ^{1}H NMR and (C) ^{13}C NMR spectra of TPEC.

were removed by vacuum rotary evaporation, and the crude product was chromatographed on silica gel with petroleum ether (60–90 °C)/ethyl acetate (1/1, v/v) as eluent to give TPE-OH as white solid. Yield = 30%.

Cyanuric chloride was conjugated on TPE-OH as described previously with some modifications.[23] Briefly, TPE-OH (166 mg, 0.419 mmol) solution in acetone (5 mL) was added dropwise to cyanuric chloride (310 mg, 1.7 mmol) and DIPEA (0.593 mL, 3.4 mmol) solution in acetone (3 mL). After stirring for 3 h at 4 °C, the mixture was concentrated by vacuum rotary evaporation, and the crude product was chromatographed on silica gel with petroleum ether (60–90 °C)/ethyl acetate (3:1, v/v) as eluent to give TPEC as light yellow powder. Yield = 69%.

2.3. Characterization of TPEC Conjugates. ^{1}H NMR and ^{13}C NMR spectra of TPE-OH and TPEC were recorded on a Bruker AM 400 apparatus (Billerica, MA), using tetramethylsilane as the internal reference. The AIE property of TPEC was examined from the fluorescence intensity change in acetone–water mixtures with different water contents as described previously.[24] Briefly, a stock solution of TPEC in THF with a concentration of 1 mM was prepared, and 0.1 mL of this solution was transferred to a 10 mL centrifuge tube. After the addition of an appropriate amount of acetone, water was dropped slowly under vigorous stirring to achieve a 10 mL mixture of acetone and water. The water content in the mixture varied in the range of 0–99 vol %, and the emission spectra of the resulting solutions and aggregates were measured by a fluorescence spectroscope (Hitachi F-7000, Japan) at the excitation and emission wavelengths of 364 and 461 nm, respectively.

2.4. Preparation of Mannose-Conjugated Fibers. PSMA fibers were prepared by electrospinning as described previously.[16] Briefly, PSMA was dissolved in dimethylformamide, THF, and acetone (2:5:3, v/v/v), followed by loading into a syringe with a stainless steel needle as the nozzle. The polymer solution was continuously pushed by a microinject pump (Zhejiang University Medical Instrument Co., Hangzhou, China) at a flow rate of 10 mL/h. The electrospinning was operated under a fixed electric field of 20 kV/15 cm, using a high-voltage statitron (Tianjing High Voltage Power Supply Co., Tianjing, China). Fibers were deposited onto an aluminum sheet wrapped around a rotating cylinder and vacuum-dried to remove residual solvent. PSMA composite fibers containing different amounts of PS were also obtained by blend electrospinning following the same procedures.

Scheme 1. (a) Schematic Drawing of the Grafting of PEG, HDA, or PEI on PSMA Fibers, Followed by TPEC Conjugation and Mannose Immobilization. (b) The Emission of Green Fluorescence of TPE after Specific Binding of FimH Proteins on the *E. coli* Surface with Mannose Grafts of TPE-Man-Grafted Fibers

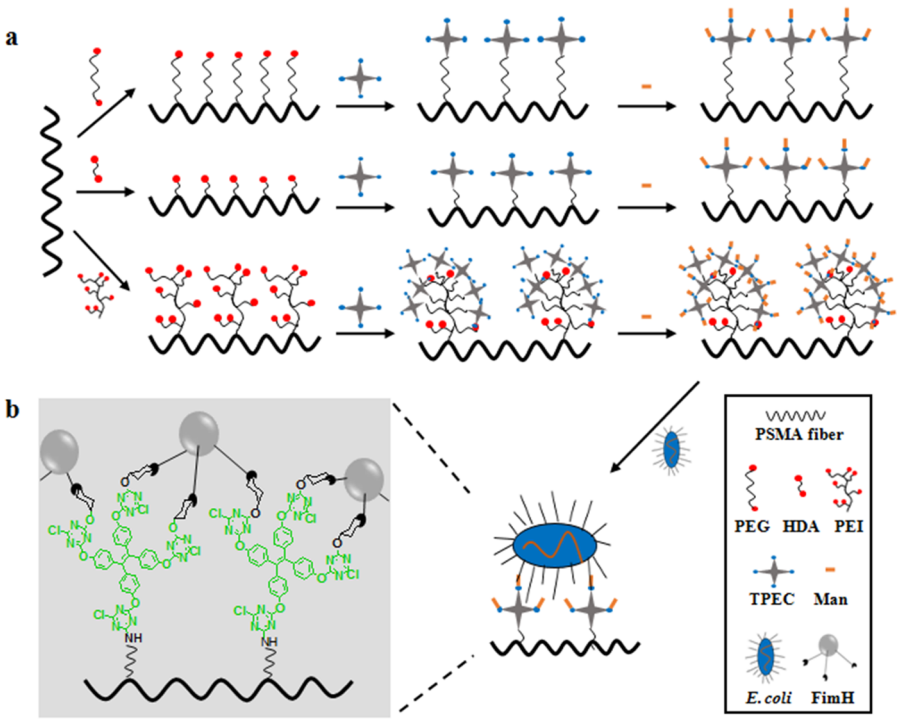

DOI: 10.1021/am507593p
ACS Appl. Mater. Interfaces 2015, 7, 5177–5186

Scheme 1a summaries the grafting process of TPE-Man on electrospun PSMA fibers using PEG as spacers. Briefly, PSMA fibers were immersed into 5 mL of PEG diamine solution (100 mg/mL) and kept under mild stirring at 25 °C for 5 h, followed by water washing and vacuum drying to obtain PSMA-PEG fibers. The aminated fibers were incubated with a mixture solution of TPEC (100 mM) and DIPEA (100 mM) in water-saturated mixtures of ethylene ether and acetonitrile (96/4, v/v), which were kept under mild stirring at room temperature for 8 h. PSMA-PEG-TPEC fibers were obtained after flushing with ether and drying under N_2 stream. Then, the fibers were immersed in 10 mL of mannose solution (30 mM, adjusted to pH 9.0 with 1 M NaOH) and incubated at room temperature for 6 h. The fibers were successively washed with distilled water and dried under N_2 stream to get PSMA-PEG-TPEC-Man fibers. Alternatively, PEI and HDA were used as spacers to prepare PSMA-PEI-TPEC-Man and PSMA-HDA-TPEC-Man fibers, respectively, following the same procedures.

2.5. Characterization of Mannose-Conjugated Fibrous Mats. The morphology of fibrous mats was observed by a scanning electron microscope (SEM; FEI Quanta 200, The Netherlands) equipped with a field emission gun (20 kV) and a Robinson detector after 2 min of gold coating to minimize the charging effect. The fiber diameter and pore size of fibrous mats were evaluated from SEM images at different fiber segments or random spots to generate an average value. The porosity of fibrous mats was determined from the apparent density compared with the bulk density of matrix polymers as described previously.[25] The water contact angle (WCA) of electrospun fibrous mats was measured on a Kruss GmbH DSA100 Mk 2 goniometer (Hamburg, Germany), followed by image processing of sessile drop with DSA 1.8 software, and the final results were obtained by averaging at least five separate runs. The AIE property of PSMA-PEG-TPEC-Man fibrous mats was examined after immersion in distilled water and hexane for 10 min. The emission spectra of the wet fibrous mats were measured immediately by a fluorescence spectrophotometer at the excitation and emission wavelengths of 364 and 461 nm, respectively.

The chemical compositions of fibers were characterized by an X-ray photoelectron spectroscope (XPS, XSAM800, Kratos Ltd., UK), taken between 50 and 1300 eV with an energy step of 0.5 eV using pass energy of 300 eV. The amino group densities of aminated fibers were determined via colorimetric methods based on Orange II binding.[26] Briefly, the aminated fibers were immersed in acidic Orange II solution (pH = 3, 3 mg/mL) for 30 min at 40 °C. Then, the fibers were intensively rinsed several times using an acidic solution (distilled water adjusted to pH 3 with 1 M HCl) until no unbound dye was detected in the washing solution. After drying under air stream, the fibers were immersed in an akaline solution (distilled water adjusted to pH 12 with 1 M NaOH) to desorb the dye. The retrieved solution containing the desorbed dye was adjusted to pH 3 by adding HCl solution. The amino group content was detected at 484 nm with an ultraviolet−visible (UV−vis) spectrophotometer (UV-2550, Shimadzu, Japan), in which the calibration curve was obtained with Orange II solutions of known concentrations.

The mannose immobilized on the surface of PSMA fibers could display their inherent recognizing ability with concanavalin A (ConA), so FITC-labeled ConA was used for a semiquantitation of the surface mannose as described previously.[23] Briefly, the mannose-conjugated PSMA fibers were cut to fit the size of a 48-well tissue culture plate. Each fibrous mat was immersed in 200 μL of Tris-HCl buffer containing 0.02 mg of FITC-labeled ConA for 1 h at 37 °C. The unbound lectin was removed after intensive rinse using a Tris-HCl buffer. Then, the bound lectin was dissociated by adding 100 μL of supersaturated mannose solution to the wells and incubated for 1 h at 37 °C.[27] The emission spectra of the resulting lectin solutions was measured immediately by a fluorescence spectrophotometer at the excitation and emission wavelengths of 492 and 518 nm, respectively, and calibrated with lectin solutions of known concentrations.

2.6. Bacterial Cultivation. In the current study, *E. coli* and *S. epidermidis* were used as testing and control bacteria, respectively, to induce the fluorescence change of TPE-Man-grafted fibrous mats. Bacteria were seeded and cultured in suspensions using Luria−Bertani (LB) media. For these bacteria, a single colony was inoculated in bacteria media at 37 °C overnight, shaking at 200 rpm. The turbid suspension was diluted with LB media to OD_{600} = 0.1, which corresponded to around 1×10^6 colony-forming units per milliliter (CFU/mL) based on colony counting on LB agar plates. The suspension was finally diluted to a desired concentration in phosphate buffer saline (PBS).

2.7. Bacteria Detection on TPEC-Man-Conjugated Fibrous Mats. PSMA-PEG-TPEC-Man fibrous mats were punched into round sections with diameter of 25 mm (around 20 mg), on which 1 mL of *E. coli* suspension in PBS (10^3 and 10^5 CFU/mL) was added. After incubation for different time periods, the fluorescence spectra of fibrous mats were measured immediately by a fluorescence spectrophotometer at the excitation and emission wavelengths of 364 and 461 nm, respectively. The bacteria-loaded fibrous mats were fixed in 4% paraformaldehyde and freeze-dried, and the distribution of bacteria on fibrous mats was observed by SEM as above. To test the specific binding between TPEC-Man grafts and *E. coli* cells, *S. epidermidis* suspensions and the mixture of *E. coli* suspension and free mannose (50 mg/mL) were also incubated with mannose-conjugated fibers. After incubation for 10 min, the emission spectra of the wet fibrous mats were measured as described above.

Bacteria suspensions with different concentrations up to 10^5 CFU/mL were tested on fibers with different spacers (PEG, HDA, or PEI) for mannose conjugation. PSMA/PS composite fibers containing up to 40% PS were grafted with TPE-Man, and the fluorescence intensities were measured on the wet fibrous mats after incubation with bacteria suspensions with different concentrations. In order to explore the interference by other proteins and carbohydrates in the bacteria detection, bacteria suspensions in PBS containing BSA (1 mg/mL), glucose (50 mg/mL), or both of them were tested following the same process.

2.8. Statistics Analysis. The statistical significance of the data obtained was analyzed by the Student's *t* test. Data are expressed as mean ± standard deviation (S.D.). Probability values of $p < 0.05$ were interpreted as denoting statistical significance.

3. RESULTS

3.1. Characterization of TPEC. TPEC was prepared by coupling cyanuric chloride on TPE-OH, which was obtained through a McMurry reaction between two molecules of 4,4′-dihydroxybenzophenone (Figure 1A). The chemical structures of TPE-OH were confirmed from ^{1}H NMR (DMSO-d_6, ppm): δ 6.48 (d, 8H) and 6.68 (d, 8H); ^{13}C NMR (DMSO-d_6, ppm): δ 114.5, 132.2, 135.5, 138.1, and 155.5. Cyanuric chloride is a heterocyclic trifunctional compound, and its most known feature is that the three chlorines on the triazine ring can be replaced stepwise by hydroxyls and/or amino groups through the regulation of reaction temperature. Another attracting feature is the potential to turn around its immobilization bond after immobilization on a solid surface,[23] which allows TPE molecules to adjust their spatial position and avoids AIE phenomena after grafting on fibers. Figure 1B shows ^{1}H NMR of TPEC, indicating absorption peaks at 7.02 (d, 8H) and 7.16 ppm (d, 8H). Compared with those of TPE-OH, the shift of these peaks confirmed the conjugation of cyanuric chloride on TPE-OH. Figure 1C shows ^{13}C NMR of TPEC as well as detailed assignment of each peak, indicating peaks at 120.6, 132.8, 140.0, 141.1, 149.7, 170.9, and 172.9 ppm. Compared with that of TPE-OH, additional peaks at 170.9 and 172.9 ppm belonged to those of cyanuric chloride.

TPE-OH exhibited typical AIE phenomena as described previously,[14] and the fluorescence properties of TPEC were determined by the addition of water into TPEC solutions.[28] As shown in Figure 2a, the photoluminescence spectra ran nearly parallel to the abscissa when TPEC was dissolved in acetone, a

DOI: 10.1021/am507593p
ACS Appl. Mater. Interfaces 2015, 7, 5177−5186

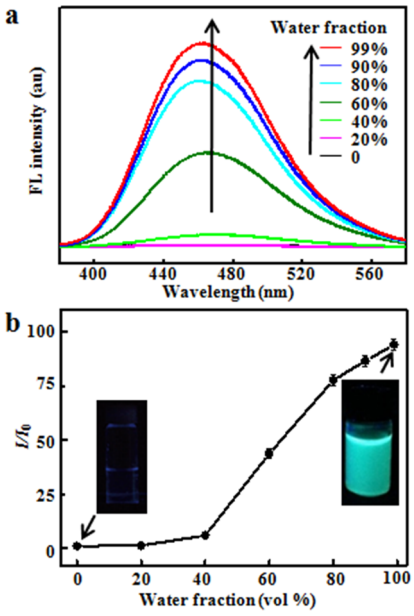

Figure 2. (a) Fluorescence spectra of TPEC in acetone in the presence of different water contents up to 99%. (b) Changes in the fluorescence intensity (I) of TPEC at 461 nm with the water fraction in the mixture of acetone and water (n = 3), and I_0 is the intensity of TPEC in acetone. Insets are photographs of TPEC in acetone and the acetone–water mixture taken at 365 nm under the illumination of a hand-held UV lamp.

good solvent for TPEC, verifying the nonemissive nature in a solution state, but the solution of TPEC in acetone emit weak green light after the addition of water to induce an aggregation of TPEC. The addition of a higher amount of water increased the green emission intensity and was progressively accompanied by a blue shift in the emission maximum, due to the increased solvent polarity.[29] As shown in Figure 2b, the fluorescence intensity became visible when large water contents of over 40% were added into the acetone solution of TPEC. As the water ratios increased from 40% to 99%, there was around a 17-fold increase in the emission intensity of TPEC in the acetone–water mixtures. As shown in the inset of Figure 2b, there were remarkable differences in the fluorescent photographs of TPEC between acetone and acetone–water mixtures, observed under an UV illumination. Therefore, the photoluminescence properties of TPEC indicated the maintenance of AIE activities after incorporating cyanuric chloride into the TPE core.

3.2. Characterization of TPE-Man-Conjugated PSMA Fibers. Figure 3 shows SEM images of PSMA and mannose-conjugated PSMA fibrous mats, displaying a common feature of being bead-free, randomly arrayed, and very porous. The average diameter of PSMA and PSMA-PEG-TEC-Man fibers mats was 0.86 ± 0.09 and 1.25 ± 0.11 μm, respectively, providing high specific surface area for bacteria binding. To increase the interaction between mannose and bacteria, PEG, PEI, or HDA was introduced as spacers between the fiber and mannose. The tether was supposed to reduce unfavorable charge and/or hydrophobic/hydrophilic interactions with the fiber surface and increase the conformational mobility of the mannose. The spacers and mannose grafts on the fibers led to water swelling of the fiber matrix and a significant increase in the fiber size. PSMA and PSMA-PEG-TEC-Man fibrous mats indicated average pore sizes of 12.1 ± 1.4 and 8.4 ± 0.9 μm and

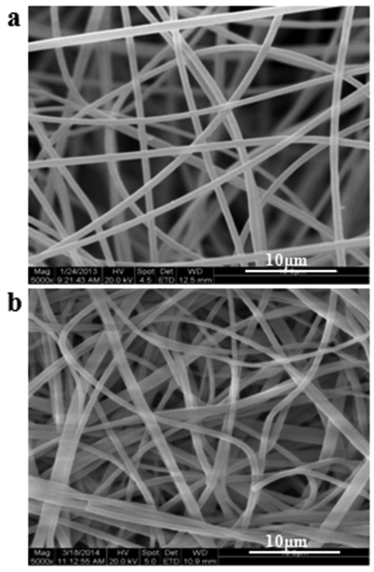

Figure 3. SEM images of (a) PSMA and (b) mannose-conjugated PSMA fibrous mats.

porosities of 92% and 81%, respectively. The WCA of PSMA fibers was around 126°, indicating a hydrophobic surface. However, a highly hydrophilic fiber surface with WCA of 0° was observed for mannose-conjugated PSMA fibrous mats.

The stepwise reaction was verified by XPS analysis on PSMA-PEG, PSMA-PEG-TPEC, and PSMA-PEG-TPEC-Man fibers. As shown in Figure 4a, a weak N 1s peak at the binding energy of around 400 eV was presented on PSMA-PEG mats, indicating PEG diamine grafts on the fiber surface. The immobilization of TPEC on the aminated fiber surface led to an obvious increase of the N 1s peak area, and a new peak

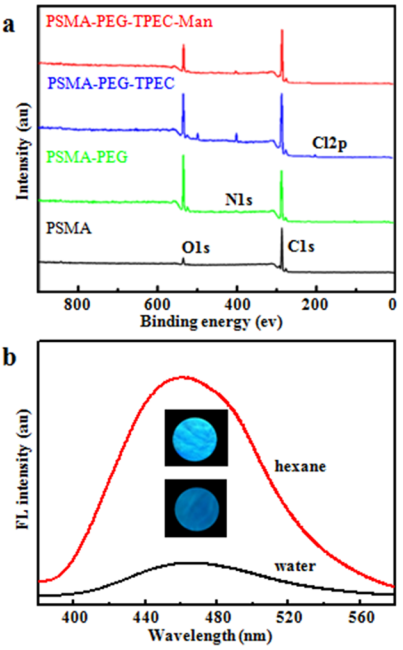

Figure 4. (a) XPS spectra of PSMA, PSAM-PEG, PSMA-PEG-TPEC, and PSMA-PEG-TPEC-Man fibers. (b) Fluorescence spectra of PSMA-PEG-TPEC-Man fibers after immersion in distilled water and hexane. Insets are photographs of the fibrous mat taken at 365 nm under the illumination of a hand-held UV lamp.

DOI: 10.1021/am507593p
ACS Appl. Mater. Interfaces 2015, 7, 5177–5186

appeared at 200.8 eV corresponding to chlorine. As expected, the chlorine signal disappeared after PSMA-PEG-TPEC fibers was further treated with a mannose solution in basic conditions, where all the unreplaced chlorine was removed by hydrolysis.[23] An evident decrease of the N 1s peak area for PSMA-PEG-TPEC-Man fibers was also observed due to the embedment of TPEC under the newly immobilized mannose. This clear evidence revealed the grafting of TPEC on PSMA-PEG fibers and the immobilization of mannose on TPEC-activated fibers.

To determine whether the fibers had the AIE activity after TPEC grafting and mannose immobilization, PSMA-PEG-TPEC and PSMA-PEG-TPEC-Man fibers were immersed in distilled water or hexane and the emission spectra were measured immediately on the retrieved wet fibrous mats. Both the fibrous mats after immersion in hexane emitted strong green fluorescence, indicating almost a 7-fold higher fluorescence intensity than those immersed in water (Figure 4b). The inset of Figure 4b shows the dramatic fluorescence contrast between these fibrous mats under an UV illumination. PEG and mannose were not dissolved in hexane, so the precipitation of PEG chains induced TPEC to aggregate on the fiber surface and enhanced the AIE intensity. Thus, the AIE activities were preserved after TPEC grafting and mannose immobilization on the fiber surface.

3.3. Fluorescence Intensities of Mannose-Conjugated PSMA Fibers in the Presence of Bacteria. The mannose-conjugated PSMA fibers were used for bacteria detection through the fluorescence changes, resulting from the restricted intramolecular motion of TPE after a specific binding between mannose and *E. coli* (Scheme 1b). All the hydroxyl groups of mannose, except 1-OH, could bind extensively with FimH protein of *E. coli*.[30] *S. epidermidis*, a Gram-positive bacterium without fimbria to bind with mannose, was used as control. As shown in Figure 5a, the emission intensity of fibrous mats after treatment with 10^3 and 10^5 CFU/mL of *S. epidermidis* indicated no significant changes compared with that before treatment. However, the mannose-conjugated fibrous mats treated with 10^3 and 10^5 CFU/mL of *E. coli* showed an almost 3- and 5-fold increase in the emission intensities, respectively. The addition of free mannose into the *E. coli* suspension was used to interrupt the specific interactions between bacteria and mannose-conjugated fibers. As expected, the fluorescence intensity of the fibrous mats was much weaker than those after incubation with *E. coli* (Figure 5a). The above data indicated that the specific recognition of mannose toward FimH protein was well conserved after anchoring on fibers by TPEC. The intense emission of fibrous mats indicated that the specific binding between *E. coli* cells and anchored mannose molecules efficiently restricted the intramolecular motion of TPE. Figure 5b shows SEM images of mannose-conjugated PSMA fibrous mats after incubation with 10^3 CFU/mL of *E. coli*, displaying a uniform distribution feature of microbes on fibers.

The fluorescence spectra of mannose-conjugated fibrous mats were detected after incubation for different time periods with *E. coli* at different concentrations. Figure 5c summarizes the fluorescence intensities of fibrous mats after incubation with *E. coli* suspensions, indicating a rapid increase during the early incubation stage. The fluorescence intensities reached a steady value after incubation with *E. coli* suspensions at both 10^3 and 10^5 CFU/mL for 10 min, which was set as the incubation time during the following tests. As shown in Figure 5d, the immersion of mannose-conjugated fibrous mats in *E. coli*

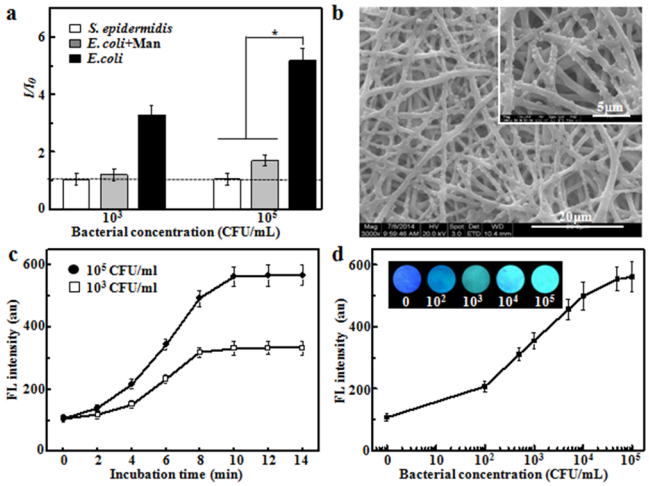

Figure 5. (a) Changes of the fluorescence intensity (I) of PSMA-PEG-TPEC-Man fibrous mats after incubation with *E. coli* and *S. epidermidis* at the concentrations of 10^3 and 10^5 CFU/mL, compared with the addition of free mannose into *E. coli* ($n = 5$). I_0 is the intensity of the fibrous mats without bacteria incubation (∗: $p < 0.05$). (b) SEM morphologies of bacteria-loaded fibrous mats. Inset shows the magnified image. (c) Fluorescence intensities of PSMA-PEG-TPEC-Man fibrous mats after incubation for up to 14 min with *E. coli* at 10^3 and 10^5 CFU/mL ($n = 5$). (d) Fluorescence intensities of fibrous mats after incubation with *E. coli* at different concentrations ($n = 5$). Inset is the color strip of fibrous mats taken at 365 nm under the illumination of a hand-held UV lamp.

suspensions resulted in fluorescence enhancement with the increase in the bacteria concentrations. The fluorescence intensity of fibrous mats was drafted against *E. coli* concentrations by statistic software of OriginPro 8.5 and expressed by the equation:

$$Y = 2.6 + 236/(1 + 10^{(60-x)\times 0.06}) \quad (R^2 = 0.994)$$

where Y represents the fluorescence intensity and X is the concentration of *E. coli* suspensions (CFU/mL). Coefficients of correlation (R^2) of the equation were relatively high, which was in agreement with the requirements of statistical analysis. Thus, the *E. coli* concentration can be obtained from a fluorescence intensity using the above equation. In addition, to achieve a visual readout for potential field use, a color strip of fibrous mats was established after immersion into *E. coli* of different concentrations. As shown in the inset of Figure 5b, the fibrous mats turned from blue to green after incubation with *E. coli* of 10^3 CFU/mL, and a bluish-green fibrous mat was shown after incubation with *E. coli* of 10^2 CFU/mL. The established color strips are useful in health care or social settings for *E. coli* determination and in monitoring the change of bacterial concentrations in real-time, where the purpose of the test is to quantify the bacteria concentration in a short time, without the need to complex experimental procedures.

3.4. Effect of Spacers for TPE-Man Conjugation on the Fluorescence Intensities of Fibers. To increase the interaction between mannose grafts on fibers with FimH proteins of *E. coli* and reduce the unfavorable charge and/or hydrophobic/hydrophilic interactions on the fiber surface, flexible molecular tethers were introduced between the fiber matrix and mannose. HDA, PEG, and PEI were amino-terminated molecules with different chain lengths. Figure 6a shows the fluorescence intensities of PSMA-HDA-TPEC-Man

DOI: 10.1021/am507593p
ACS Appl. Mater. Interfaces 2015, 7, 5177−5186

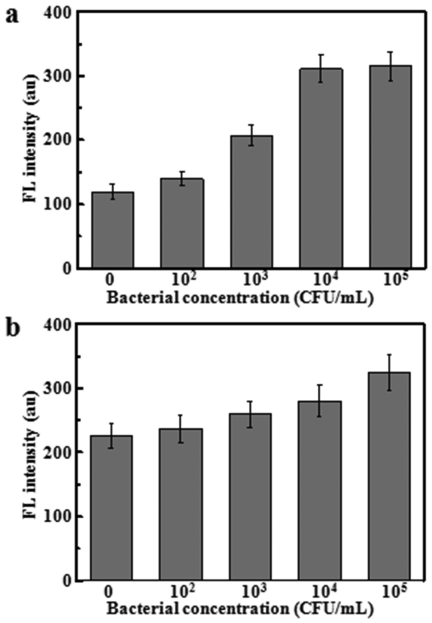

Figure 6. Fluorescence intensities of (a) PSMA-HDA-TPEC-Man and (b) PSMA-PEI-TPEC-Man fibrous mats after incubation with *E. coli* at different concentrations (n = 5).

fibrous mats under different *E. coli* concentrations. Compared with fibrous mats without bacteria treatment, there was no significant change in the fluorescence intensity when the *E. coli* concentration was 10^2 CFU/mL ($p > 0.05$). Although the fluorescence intensity of PSMA-HDA-TPEC-Man fibers increased slightly when the *E. coli* concentration was increased to 10^3 CFU/mL, the enhancement of fluorescence intensity was still not obvious. As shown in Figure 6a, there was around a 3-fold increase in the fluorescence intensity after immersion of PSMA-HDA-TPEC-Man fibers with 10^4 CFU/mL of *E. coli* and no more increase after incubation with 10^5 CFU/mL bacteria. This data indicated that the saturation value of PSMA-HDA-TPEC-Man fibers for *E. coli* detection was around 10^4 CFU/mL. HDA tethers were much shorter than PEG and could not provide enough space for mannose terminals to specifically bind with bacteria.

Figure 6b shows the relationship of *E. coli* concentrations and fluorescence intensities of PSMA-PEI-TPEC-Man fibers. The enhancement of the fluorescence intensity with the increase in the bacteria concentration was less significant compared with mannose-conjugated fibers using PEG and HDA as tethers. The fluorescence intensity of PSMA-PEI-TPEC-Man fibers without bacteria incubation was significantly larger than that of PSMA-PEG-TPEC-Man fibers ($p < 0.05$). Due to a large amount of amino groups exposed on the surface of PSMA-PEI-TPEC-Man fibers, the reaction sites between TPEC and PSMA-PEI were much richer than those of PSMA-PEG. A high density or multiple point conjugation of TPEC on the fiber surface was supposed to produce spatial hindrance for TPEC themselves and induce the restriction of intramolecular motion, leading to the high fluorescence intensities of PSMA-PEI-TPEC-Man fibers without bacteria incubation. In addition, due to the high density and self-aggregation of TPE-Man on the fiber surface, even a large amount of FimH proteins was bound with mannose, and there was no significant enhancement of the fluorescence intensity (Figure 6b). As indicated above, compared with the use of HDA and PEI as spacers for TPE-Man grafting, PSMA-PEG-TPEC-Man fibers indicated a sensitive change in the fluorescence intensities against bacteria concentrations, a lower fluorescence background of fibers without bacteria incubation, and a sufficient binding space with bacteria of higher concentrations.

3.5. Effect of Mannose-Grafting Densities on the Fluorescence Intensities of Fibers. In order to adjust the mannose densities on the surface of PSMA fiber, different amounts of PS were mixed with PSMA for blend electrospinning at PSMA/PS ratios of 100/0, 95/5, 90/10, 85/15, 80/20, and 60/40 (w/w). Figure 7a shows the densities of amino

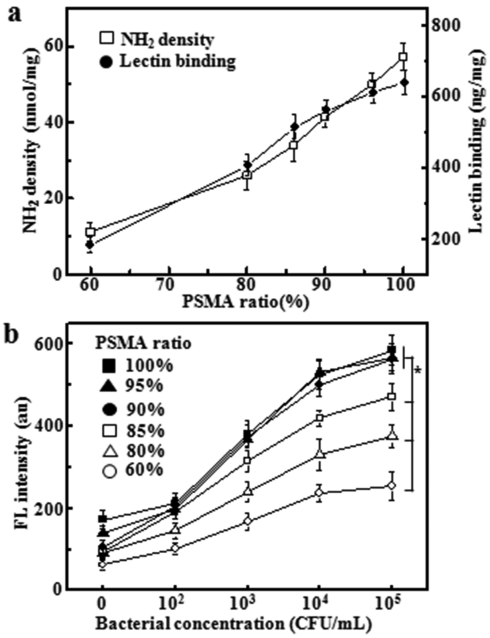

Figure 7. (a) Amino group densities and lectin binding amounts on the surface of PSMA/PS fibers with different amounts of PSMA after grafting with PEG diamine (n = 3). (b) Fluorescence intensities of PSMA/PS fibers with different amounts of PSMA after incubation with *E. coli* at different concentrations (n = 5; *: $p < 0.05$).

groups on the surface of PSMA/PS fibers after grafting with PEG diamine. The increase in PS contents in fibers led to a drastic reduction of amino group densities on the fiber surface. The amino group density on the surface of PSMA/PS fibers containing 60% PSMA was just 18% of that of PSMA fibers, due to the enrichment of chemical groups with low binding energy on the surface of electrospun fibers.[31] The amount of mannose exposed on the fiber surface was semiquantified by using a specific binding activity with ConA as described previously.[23] As shown in Figure 7a, the increase in the amount of lectin binding was similar to that of amino group densities on the fiber surface, indicating that TPE-Man has been sufficiently conjugated on the aminated fiber surface.

Figure 7b shows the fluorescence intensities of PSMA/PS fibers with different mannose densities after incubation with bacteria. The higher mass ratios of PSMA in fibers led to significantly higher fluorescence intensities after treatment with *E. coli* suspensions ($p < 0.05$), due to the specific binding between FimH proteins and TPE-Man grafts with higher densities. However, when the mass ratio of PSMA increased to over 90%, the fluorescence intensities indicated no significant increase after incubation with *E. coli* of different concentrations ($p > 0.05$). As shown in Figure 7a, the mannose densities on

DOI: 10.1021/am507593p
ACS Appl. Mater. Interfaces 2015, 7, 5177−5186

the fiber surface indicated a less significant increase with PSMA ratios of over 90%, resulting in saturated interactions between bacteria and mannose grafts and no significant change in the fluorescence intensities.

3.6. Anti-interference Capability of Fibers for *E. coli* Detection. In the current study, the special interactions between mannose grafts on fibers with fimbria proteins resulted in the fluorescence intensity changes of fibrous mats, which can be used for bacteria screening in water and biological fluids. Thus, BSA and glucose were chosen as interference factors of protein and saccharides, respectively, to explore the anti-interference capability. As shown in Figure 8, the addition of

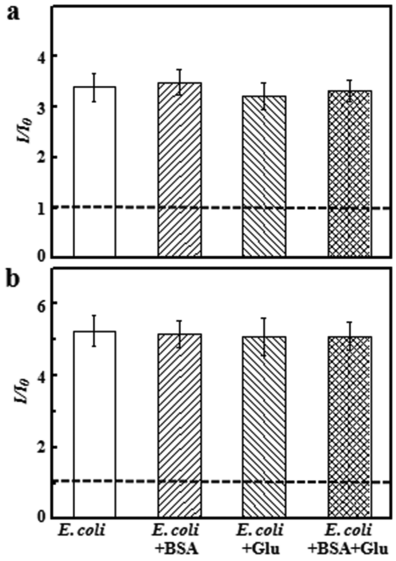

Figure 8. Fluorescence intensities (I) of PSMA-PEG-TPEC-Man fibrous mats after incubation with *E. coli* at the concentrations of (a) 10^3 and (b) 10^5 CFU/mL in the presence of BSA, glucose, or both of them (n = 5). I_0 is the intensity of the fibrous mats without bacteria incubation.

BSA, glucose, or both of them into bacteria suspensions led to no significant changes in the fluorescence intensities of fibrous mats ($p > 0.05$), and similar profiles were obtained under bacteria suspensions of both 10^3 and 10^5 CFU/mL. It was indicated that the special binding between TPE-Man grafts and FimH proteins was not subject to the interference by these proteins and saccharides.

4. DISCUSSION

There are several key issues in the design of effective sensors for pathogen detection. Currently available tests usually require complex sample preparation, and the standard detection process of bacteria takes over 24 h to obtain results.[18] Therefore, an analysis method is highly preferred on the basis of the whole bacterium without going through complex pre-enrichment preparations and a visual readout without using expensive instrumentation and experienced personnel.[14] To address these issues, test strips were established on mannose-conjugated fibrous mats in the current study for *E. coli* determination. The test strip format is useful in health care or social settings where the purpose of the test is to determine whether the bacteria concentration is within the acceptance criteria in a short time, without the need to get an exact concentration reading. Furthermore, the color strips can serve as a self-test device for the general public to monitor the amount of bacteria in an aquatic environment and can also be placed in an aqueous environment to monitor the change of bacterial concentrations in real-time.

The limit of detection (LOD) is another crucial factor, since even a few bacteria in aqueous solution may lead to a serious health risk. Environmental testing or clinical application usually requires a LOD of 10^4–10^2 cells/mL, so the research into bacterial detection aims to achieve ultrasensitive detection in complex aqueous solutions.[32] Miranda et al. developed cationic gold nanoparticles with electrostatically bound β-galactosidase, and the presence of bacteria released the enzyme with concomitant restoration of activity. An enzyme-amplified colorimetric readout was able to quantify bacteria at concentrations of 1×10^2 bacteria/mL in solution and 1×10^4 bacteria/mL in a field-friendly test strip format.[7] Lee et al. developed magnetic nanoparticles functionalized with vancomycin, which could be specifically bound with D-alanyl-D-alanine moieties in the bacterial cell wall. These molecular interactions with magnetic nanoparticles were amplified using a miniaturized diagnostic magnetic resonance system, which was able to detect 10^3 cells/mL of *Staphylococcus aureus* as a model organism.[6] In the current study, a sensitive assay based on TPE-Man-conjugated PSMA fibers exhibited a detection limit of 10^2 CFU/mL against *E. coli* cells in both fluorescence measuring and test strip format.

One reason is the use of the AIE strategy from TPE derivatives based on the restriction of intramolecular motion of benzene rings. Although a significant number of conventional fluorescence methods for detection of *E. coli* is available at the present time, these methods are still slightly problematic due to aggregation-caused quenching and poor photostability.[33] To date, fluorescent probes rarely detect bacteria at concentrations of about 10^2 CFU/mL on whole-bacterium detection without bacterial pre-enrichment of the sample.[32] El-Boubbou et al. constructed magnetic nanoparticles with mannose grafts, and the specific binding between *E. coli* and mannose was utilized to remove bacteria from suspension. The retrieved bacteria were stained with a fluorescent dye (PicoGreen), and the fluorescent microscopic imaging showed that *E. coli* could be reliably detected with a limit of 10^4 cells/mL.[30] Li et al. present a fluorescence turn-off strategy based on the AIE effect though polyelectrolyte micelles containing negatively charged multivalent TPE sulfonate derivatives, which was depleted after a competitive electrostatic binding with the bacteria surface. The disintegration of micelle structures and loss of AIE effect led to a decrease of the fluorescence emission intensity, exhibiting a detection limit of 5.5×10^4 CFU/mL against *E. coli* cells.[14]

Another reason is the unique nanostructure of electrospun fibers. Li et al. developed sialyllactose-grafted chitosan fibers to efficiently remove virus from an aqueous medium, indicating the potential function of electrospun fibrous mats as virus adsorbents for prevention and control of influenza.[34] In the current study, the highly porous structure of electrospun fibrous mats was supposed to filter the bacteria suspension and entrap the cells within the mats. The large contact area and highly hydrophilic surface were supposed to enhance the interaction between *E. coli* and mannose anchored on PSMA fibers through flexible spacers (Figure 5b). In addition, the specific binding between mannose groups and target lectin has been used as an intelligent probe for highly selective protein sensing and bacteria recognition.[35,36] In the current study, the specific binding of mannose to FimH proteins of *E. coli* induced

DOI: 10.1021/am507593p
ACS Appl. Mater. Interfaces 2015, 7, 5177–5186

a turn-on fluorescence enhancement of TPE on the fibrous mats. The resulting test strip format provided a potential tool with a visual sensitivity of bacteria concentrations as low as 10^2 CFU/mL in a matter of minutes. It should be also noted the interactions between mannose and one type of fimbria protein of Gram-negative bacteria were utilized in the current study, and the detection was not interfered by Gram-positive bacteria without fimbria and in the presence of BSA and glucose. These results have shown the capacity of electrospun fibrous mats for bioanalysis and biosensing of bacteria, and efforts are ongoing to improve the sensitivity and specificity and to transfer this methodology to multiple detection and identification strategies for general applications.

5. CONCLUSION

TPE-Man was successfully grafted onto PSMA fibers to establish *E. coli* detection and quantitation in aqueous media by making use of the AIE effect. When exposed to bacterial cells, the specific binding between mannose on the TPE-Man-conjugated fibers and FimH proteins of *E. coli* was accompanied by a remarkable increase of TPE fluorescence emission. An equation was drafted of the fluorescence intensities of fibrous mats against *E. coli* concentrations ranging from 10^2 to 10^5 CFU/mL. The test strip format was established on TPE-Man-conjugated PSMA fibers after exposure to *E. coli* of different concentrations, providing a potential tool with a visual sensitivity of bacteria concentrations as low as 10^2 CFU/mL in a matter of minutes. This novel TPE-Man conjugated fiber shows great potential for use as a simple and rapid detection system of *E. coli*. This strategy may offer a capacity to be expanded to exploit electrospun fibrous mats and other carbohydrate−cell interactions for bioanalysis and biosensing of pathogenic bacteria.

AUTHOR INFORMATION

Corresponding Author

*E-mail: xhli@swjtu.edu.cn. Tel: +8628-87634068. Fax: +8628-87634649.

Notes

The authors declare no competing financial interest.

ACKNOWLEDGMENTS

This work was supported by National Natural Science Foundation of China (21274117 and 31470922), Specialized Research Fund for the Doctoral Program of Higher Education (20120184110004), and National Scientific and Technical Supporting Programs (2012BAI17B06).

REFERENCES

(1) Shuman, E. K. Global Climate Change and Infectious Diseases. *N. Engl. J. Med.* **2010**, *362*, 1061−1063.

(2) So, H. M.; Park, D. W.; Jeon, E. K.; Kim, Y. H.; Kim, B. S.; Lee, C. K.; Choi, S. Y.; Kim, S. C.; Chang, H.; Lee, J. O. Detection and Titer Estimation of *Escherichia coli* Using Aptamer-Functionalized Single-Walled Carbon-Nanotube Field-Effect Transistors. *Small* **2008**, *4*, 197−201.

(3) Lazcka, O.; Del Campo, F. J.; Munoz, F. X. Pathogen Detection: A Perspective of Traditional Methods and Biosensors. *Biosens. Bioelectron.* **2007**, *22*, 1205−1217.

(4) Ray, P. C.; Khan, S. A.; Singh, A. K.; Senapati, D.; Fan, Z. Nanomaterials for Targeted Detection and Photothermal Killing of Bacteria. *Chem. Soc. Rev.* **2012**, *41*, 3193−3209.

(5) Ravindranath, S. P.; Mauer, L. J.; Deb-Roy, C.; Irudayaraj, J. Biofunctionalized Magnetic Nanoparticle Integrated Mid-Infrared Pathogen Sensor for Food Matrixes. *Anal. Chem.* **2009**, *81*, 2840−2846.

(6) Lee, H.; Sun, E.; Ham, D.; Weissleder, R. Chip-NMR Biosensor for Detection and Molecular Analysis of Cells. *Nat. Med.* **2008**, *14*, 869−874.

(7) Miranda, O. R.; Li, X. N.; Garcia-Gonzalez, L.; Zhu, Z. J.; Yan, B.; Bunz, U. H. F.; Rotello, V. M. Colorimetric Bacteria Sensing Using a Supramolecular Enzyme-Nanoparticle Biosensor. *J. Am. Chem. Soc.* **2011**, *133*, 9650−9653.

(8) Phillips, R. L.; Miranda, O. R.; You, C. C.; Rotello, V. M.; Bunz, U. H. F. Rapid and Efficient Identification of Bacteria Using Gold-Nanoparticle−Poly(*para*-phenylene ethynylene) Constructs. *Angew. Chem., Int. Ed.* **2008**, *47*, 2590−2594.

(9) Zhang, X. Q.; Liu, M. Y.; Yang, B.; Zhang, X. Y.; Wei, Y. Tetraphenylethene-Based Aggregation-Induced Emission Fluorescent Organic Nanoparticles: Facile Preparation and Cell Imaging Application. *Colloids Surf., B* **2013**, *112*, 81−86.

(10) Ding, D.; Li, K.; Liu, B.; Tang, B. Z. Bioprobes Based on AIE Fluorogens. *Acc. Chem. Res.* **2013**, *46*, 2441−2453.

(11) Qin, A. J.; Lam, J. W. Y.; Tang, L.; Jim, C. K. W; Zhao, H.; Sun, J. Z.; Tang, B. Z. Polytriazoles with Aggregation-Induced Emission Characteristics: Synthesis by Click Polymerization and Application as Explosive Chemosensors. *Macromolecules* **2009**, *42*, 1421−1424.

(12) Tong, H.; Hong, Y. N.; Dong, Y. Q.; Haussler, M.; Lam, J. W. Y.; Li, Z.; Guo, Z. F.; Guo, Z. H.; Tang, B. Z. Fluorescent "Light-Up" Bioprobes Based on Tetraphenylethylene Derivatives with Aggregation-Induced Emission Characteristics. *Chem. Commun.* **2006**, *35*, 3705−3707.

(13) Kato, T.; Kawaguchi, A.; Nagata, K.; Hatanaka, K. Development of Tetraphenylethylene-Based Fluorescent Oligosaccharide Probes for Detection of Influenza Virus. *Biochem. Biophys. Res. Commun.* **2010**, *394*, 200−204.

(14) Li, Y. M.; Hu, X. L.; Tian, S. D.; Li, Y.; Zhang, G. Q.; Zhang, G. Y.; Liu, S. Y. Polyion Complex Micellar Nanoparticles for Integrated Fluorometric Detection and Bacteria Inhibition in Aqueous Media. *Biomaterials* **2014**, *35*, 1618−1626.

(15) Greiner, A.; Wendorff, J. H. Electrospinning: A Fascinating Method for the Preparation of Ultrathin Fibres. *Angew. Chem., Int. Ed.* **2007**, *46*, 5670−5703.

(16) Zhao, L.; Liu, Q. J.; Yan, S. L.; Chen, Z. J.; Chen, J. M.; Li, X. H. Multimeric Immobilization of Alcohol Oxidase on Electrospun Fibers for Valid Tests of Alcoholic Saliva. *J. Biotechnol.* **2013**, *168*, 46−54.

(17) Zhu, J.; Sun, G. Lipase Immobilization on Glutaraldehyde-Activated Nanofibrous Membranes for Improved Enzyme Stabilities and Activities. *React. Funct. Polym.* **2012**, *72*, 839−845.

(18) Luo, Y. L.; Nartker, S.; Wiederoder, M.; Miller, H.; Hochhalter, D.; Drzal, L. T.; Alocilja, E. C. Novel Biosensor Based on Electrospun Nanofiber and Magnetic Nanoparticles for the Detection of *E. coli* O157:H7. *IEEE Trans. Nanotechnol.* **2012**, *11*, 676−681.

(19) Trungkathan, S.; Polpanich, D.; Smanmoo, S.; Tangboriboonrat, P. Magnetic Polymeric Nanoparticles Functionalized by Mannose-Rhodamine Conjugate for Detection of *E. coli*. *J. Appl. Polym. Sci.* **2014**, *131*, 40012 (1−9).

(20) Sharon, N. Carbohydrates as Future Anti-Adhesion Drugs for Infectious Diseases. *Biochim. Biophys. Acta, Gen. Subj.* **2006**, *1760*, 527−537.

(21) Xue, C.; Velayudham, S.; Johnson, S.; Saha, R.; Smith, A.; Brewer, W.; Murthy, P.; Bagley, S. T.; Liu, H. Highly Water-Soluble, Fluorescent, Conjugated Fluorene-Based Glycopolymers with Poly(ethylene glycol)-Tethered Spacers for Sensitive Detection of *Escherichia coli*. *Chem.—Eur. J.* **2009**, *15*, 2289−2295.

(22) Liu, L.; Zhang, G. X.; Xiang, J. F.; Zhang, D. Q.; Zhu, D. B. Fluorescence "Turn On" Chemosensors for Ag^+ and Hg^{2+} Based on Tetraphenylethylene Motif Featuring Adenine and Thymine Moieties. *Org. Lett.* **2008**, *10*, 4581−4584.

(23) Liang, K.; Chen, Y. Elegant Chemistry to Directly Anchor Intact Saccharides on Solid Surfaces Used for the Fabrication of Bioactivity-

DOI: 10.1021/am507593p
ACS Appl. Mater. Interfaces 2015, 7, 5177−5186

Conserved Saccharide Microarrays. *Bioconjugate Chem.* **2012**, *23*, 1300−1308.
(24) Hu, R. R.; Ye, R. Q.; Lam, J. W. Y.; Li, M.; Leung, C. W. T.; Tang, B. Z. Conjugated Polyelectrolytes with Aggregation-Enhanced Emission Characteristics: Synthesis and Their Biological Applications. *Chem.—Asian J.* **2013**, *8*, 2436−2445.
(25) Zhu, X. L.; Cui, W. G.; Li, X. H.; Jin, Y. Electrospun Fibrous Mats with High Porosity as Potential Scaffolds for Skin Tissue Engineering. *Biomacromolecules* **2008**, *9*, 1795−1801.
(26) Noel, S.; Liberelle, B.; Robitaille, L.; De Crescenzo, G. Quantification of Primary Amine Groups Available for Subsequent Biofunctionalization of Polymer Surfaces. *Bioconjugate Chem.* **2011**, *22*, 1690−1699.
(27) Yoon, J. J.; Nam, Y. S.; Kim, J. H.; Park, T. G. Surface Immobilization of Galactose onto Aliphatic Biodegradable Polymers for Hepatocyte Culture. *Biotechnol. Bioeng.* **2002**, *78*, 1−10.
(28) Tang, L.; Jin, J. K.; Qin, A. J.; Yuan, W. Z.; Mao, Y.; Mei, J.; Sun, J. Z.; Tang, B. Z. A Fluorescent Thermometer Operating in Aggregation-Induced Emission Mechanism: Probing Thermal Transitions of PNIPAM in Water. *Chem. Commun.* **2009**, *33*, 4974−4976.
(29) Ding, D.; Goh, C. C.; Feng, G. X.; Zhao, Z. J.; Liu, J.; Liu, R. R.; Tomczak, N.; Geng, J. L.; Tang, B. Z.; Ng, L. G. Ultrabright Organic Dots with Aggregation-Induced Emission Characteristics for Real-Time Two-Photon Intravital Vasculature Imaging. *Adv. Mater.* **2013**, *25*, 6083−6088.
(30) El-Boubbou, K.; Gruden, C.; Huang, X. Magnetic Glyconanoparticles: A Unique Tool for Rapid Pathogen Detection, Decontamination, and Strain Differentiation. *J. Am. Chem. Soc.* **2007**, *129*, 13392−13393.
(31) Cui, W. G.; Li, X. H.; Zhou, S. B.; Weng, J. Degradation Patterns and Surface Wettability of Electrospun Fibrous Mats. *Polym. Degrad. Stab.* **2008**, *93*, 731−738.
(32) Sanvicens, N.; Pastells, C.; Pascual, N.; Marco, M. P. Nanoparticle-Based Biosensors for Detection of Pathogenic Bacteria. *TrAC, Trends Anal. Chem.* **2009**, *28*, 1243−1252.
(33) Zhao, E.; Hong, Y.; Chen, S.; Leung, C. W. T.; Chan, C. Y. K.; Kwok, R. T. K.; Lam, J. W. Y.; Tang, B. Z. Highly Fluorescent and Photostable Probe for Long-Term Bacterial Viability Assay Based on Aggregation-Induced Emission. *Adv. Healthcare Mater.* **2014**, *3*, 88−96.
(34) Li, X. B.; Wu, P. X.; Gao, G. F.; Cheng, S. H. Carbohydrate-Functionalized Chitosan Fiber for Influenza Virus Capture. *Biomacromolecules* **2011**, *12*, 3962−3969.
(35) Wang, L. H.; Pu, K. Y.; Li, J.; Qi, X. Y.; Li, H.; Zhang, H.; Fan, C. H.; Liu, B. A Graphene−Conjugated Oligomer Hybrid Probe for Light-Up Sensing of Lectin and *Escherichia Coli*. *Adv. Mater.* **2011**, *23*, 4386−4391.
(36) Pu, K. Y.; Shi, J. B.; Wang, L. H.; Cai, L. P.; Wang, G.; Liu, B. Mannose-Substituted Conjugated Polyelectrolyte and Oligomer as an Intelligent Energy Transfer Pair for Label-Free Visual Detection of Concanavalin A. *Macromolecules* **2010**, *43*, 9690−9697.

DOI: 10.1021/am507593p
ACS Appl. Mater. Interfaces 2015, 7, 5177−5186